Published OnlineFirst June 25, 2019; DOI: 10.1158/0008-5472.CAN-18-3657

Tumor Biology and Immunology

Cancer Research

Activation of the VEGFC/VEGFR3 Pathway Induces Tumor Immune Escape in Colorectal Cancer

Carlotta Tacconi[1,2], Federica Ungaro[1,3], Carmen Correale[1,3], Vincenzo Arena[4], Luca Massimino[5], Michael Detmar[2], Antonino Spinelli[3,6], Michele Carvello[3,6], Massimiliano Mazzone[7,8], Ana I. Oliveira[7,8], Federica Rubbino[1,3], Valentina Garlatti[1,3], Salvatore Spanò[1,3], Enrico Lugli[9,10], Federico S. Colombo[10], Alberto Malesci[11,12], Laurent Peyrin-Biroulet[13], Stefania Vetrano[1,3], Silvio Danese[1,3], and Silvia D'Alessio[1,3]

Abstract

Colorectal cancer is a major cause of cancer-related death in Western countries and is associated with increased numbers of lymphatic vessels (LV) and tumor-associated macrophages (TAM). The VEGFC/VEGFR3 pathway is regarded as the principal inducer of lymphangiogenesis and it contributes to metastases; however, no data are available regarding its role during primary colorectal cancer development. We found that both VEGFC and VEGFR3 were upregulated in human nonmetastatic colorectal cancer, with VEGFR3 expressed on both LVs and TAMs. With the use of three different preclinical models of colorectal cancer, we also discovered that the VEGFC/VEGFR3 axis can shape both lymphatic endothelial cells and TAMs to synergistically inhibit antitumor immunity and promote primary colorectal cancer growth. Therefore, VEGFR3-directed therapy could be envisioned for the treatment of nonmetastatic colorectal cancer.

Significance: The prolymphangiogenic factor VEGFC is abundant in colorectal cancer and activates VEGFR3 present on cancer-associated macrophages and lymphatic vessels; activation of VEGFR3 signaling fosters cancer immune escape, resulting in enhanced tumor growth.

Introduction

Colorectal cancer is one of the major causes of cancer-related mortality in the Western countries. Standard treatments for colorectal cancer comprise surgery, chemotherapy, and targeted therapy, however with limited efficacy (1). In addition to poor treatment availability, approximately 40% of the surgically cured patients will experience cancer recurrence within 5 years. The tumor microenvironment is a complex network of cells and molecules that evolves with and provides support for cancer development and transition to malignancy. In the tumor context, immune surveillance may be inhibited during cancer development by the release of cytokines, chemokines, and growth factors, which all together can induce immune tolerance. Developing tumors require increasing amounts of nutrients and oxygen; in fact, both blood and lymphatic networks expand, undergoing angiogenesis and lymphangiogenesis, respectively. We have recently demonstrated that active lymphangiogenesis takes place in colorectal cancer and mediates its metastatic process (2). The expansion of lymphatic vessels (LV) can be induced in response to the activation of the VEGF receptor 3 (VEGFR3) by its ligand VEGF C (VEGFC), which is abundant in advanced stages of colorectal cancer (2). In fact, the VEGFC/VEGFR3 pathway is considered as the main inducer of lymphatic endothelial cell proliferation, migration, and survival, which in adulthood takes place during inflammation, tissue repair, and cancer (3). However, lymphatic endothelial cells (LEC) have recently been proposed to modulate the antitumoral adaptive immune response (4–6), suggesting a new role for LVs in antitumor immunity. More in detail, LVs were shown to upregulate the programmed cell death ligand-1 (PD-L1), an immune checkpoint protein, both at the primary tumor site (4) and in draining lymph nodes (5), ultimately triggering T-cell exhaustion.

[1]Laboratory of Gastrointestinal Immunopathology, Humanitas Clinical and Research Center, Rozzano, Italy. [2]Institute of Pharmaceutical Sciences, Swiss Federal Institute of Technology, Zurich, Switzerland. [3]Department of Biomedical Sciences, Humanitas University, Pieve Emanuele, Italy. [4]Department of Internal Medicine, Catholic University of Rome, Rome, Italy. [5]School of Medicine and Surgery, University of Milan-Bicocca, Milan, Italy. [6]Colon and Rectal Surgery Department, Humanitas Research Hospital, Rozzano, Italy. [7]Laboratory of Tumor Inflammation and Angiogenesis, Center for Cancer Biology, Leuven, Belgium. [8]Lab of Tumor Inflammation and Angiogenesis, Department of Oncology, KU Leuven, Leuven, Belgium. [9]Laboratory of Translational Immunology, Humanitas Clinical and Research Center, Rozzano, Italy. [10]Humanitas Flow Cytometry Core, Humanitas Clinical and Research Center, Rozzano, Italy. [11]Department of Biotechnologies and Translational Medicine, University of Milan, Rozzano (Milan), Italy. [12]Department of Gastroenterology, Humanitas Clinical and Research Center, Rozzano (Milan), Italy. [13]Institut National de la Santé et de la Recherche Médicale U954 and Department of Gastroenterology, Nancy University Hospital, Lorraine University, Nancy, France.

Note: Supplementary data for this article are available at Cancer Research Online (http://cancerres.aacrjournals.org/).

S. Danese and S. D'Alessio are the cosenior authors of this article.

Corresponding Author: Silvia D'Alessio, Humanitas University, Via Rita Levi Montalcini 4, Pieve Emanuele 20090, Italy. Phone: 390-2822-5205; Fax: 3902-8224-5101; E-mail: silvia.dalessio@hunimed.eu

Cancer Res 2019;79:4196–210

doi: 10.1158/0008-5472.CAN-18-3657

©2019 American Association for Cancer Research.

Downloaded from cancerres.aacrjournals.org on February 26, 2020. © 2019 American Association for Cancer Research.

Published OnlineFirst June 25, 2019; DOI: 10.1158/0008-5472.CAN-18-3657

In addition to LVs, immune cells are also profoundly changed during cancer development (6). Among leukocytes, macrophages are highly recruited at the tumor site and remain present at all stages of cancer progression (7). Tumor-associated macrophages (TAM) can exert immunosuppressive activity through the expression of a wide range of molecules, such as inducible nitric oxide (iNOS), arginase-1, IDO and IL10 (8–11), or by blocking T-cell proliferation and cytotoxic activity. VEGFR3 was found to be expressed by a substantial fraction of peripheral blood monocytes and activated tissue macrophages (12–14). Importantly, macrophages can directly respond to the VEGFC/VEGFR3 pathway, acquiring a hybrid phenotype that expresses both classically activated (M1) and alternatively activated (M2) molecules (12) and closely resembles TAM features (11). So far, the role of the VEGFC/VEGFR3 pathway in tumors has mainly been associated with the metastatic process; only few studies, which reported controversial results, have shown a contribution of VEGFR3 signaling in primary tumor formation and growth (5, 13, 15, 16). Here, we investigated for the first time the involvement of the VEGFC/VEGFR3 pathway in colorectal cancer development and growth, focusing on the characterization of both tumor-associated LVs and TAMs and how these cell types respond to VEGFR3 signaling, influencing antitumor immunity.

Materials and Methods

Tumor models

Sporadic colon cancer was induced by a single intraperitoneal injection of azoxymethane (AOM, 10 mg/kg, Sigma-Aldrich) in 7-week-old C57BL/6 female mice and kept on regular water for 7 days. After 7 days, mice were subjected to four oral cycles of 2.5% DSS (molecular mass, 40 kDa, MP Biomedicals), each characterized by 5 days of DSS exposure in drinking water ad libitum. The DSS cycles were interspersed with 1 week of normal drinking water. Mice were sacrificed after 50 days from the first DSS exposure. Colitis severity was scored using a disease activity index (DAI) score based on daily evaluation of body weight, diarrhea, and presence of blood in stools (12). Scoring of tumor development was based on tumor size and the number of tumors, as described previously (17). Grading of intestinal inflammation and mucosal lesions (glandular intraepithelial neoplasia and low-grade and high-grade adenomas) were evaluated histologically in a blinded fashion by an experienced pathologist.

Eight-week-old male BALB/c immunocompetent or female C57BCL6 mice were anesthetized with 100 mg/kg ketamine and 50 mg/kg xylazine. With the use of a 29-gauge syringe, 4×10^5 CT26 cells or 2×10^5 MC38 cells were injected submucosally into the distal posterior rectum in a final volume of 50 μL, as described previously (2). Tumor growth was visually monitored daily. Before being sacrificed mice bearing mCherry CT26–positive tumors were anesthetized with 100 mg/kg ketamine and 50 mg/kg xylazine and fluorescent imaging was performed using a Caliper Xenogen IVIS Spectrum (Caliper Life Sciences). After animals' sacrifice, tumors were measured by a digital caliper measuring tumor length, width, and height and were weighted using a digital scale. Procedures involving mice conformed to institutional guidelines in agreement with national and international law and were approved by the ethics committee of the Humanitas Research Hospital with the project number 13/2013 approved by the Ministry of Health.

Macrophage depletion

Mice were given BLZ945 (Sellekchem, S7725) formulated in 4% DMSO + 30% PEG 300 (Sigma) + ddH20 at a concentration of 2.5 mg/mL. Mice received 200 mg BLZ945 per kg of bodyweight or vehicle [4% DMSO + 30% PEG 300 (Sigma) + ddH20] by oral gavage once daily starting 5 days before tumor cells injection and throughout the experiment.

Vaccination studies

Mice were immunized via the intrarectal route using a disposable feeding needle as described previously with slight modifications (18). Briefly, mice were anesthetized with ketamine/xylazine on days −14, −7, and +7 from the date of tumor cells injection and were given a rectal infusion of 100 μg of OVA (Sigma Aldrich) and 10 μg of LPS (Sigma Aldrich) in a final volume of 50 μL (18). As controls, mice were administered with LPS alone.

Quantification and statistical analysis

Statistical analyses were performed using GraphPad Prism 7 (GraphPad Software). Data were presented as means ± SD or ± SEM and differences were considered statistically significant when $P < 0.05$. More in details, for experiments where there are only two groups a *t* test was applied, for experiments including more groups and/or more time points an ANOVA multivariate analysis was performed accompanied by a *post hoc* modification test as described in Figure legends.

Results

The VEGFC/VEGFR3 pathway is upregulated in colorectal cancer and positively correlates with LV and macrophage density

To investigate the involvement of the VEGFC/VEGFR3 pathway in colorectal cancer onset, we took advantage of the Gene Expression Across Normal and Tumor tissue (GENT) database (http://medicalgenome.kribb.re.kr/GENT/search/search.php). Gene expression profiles of more than 200 patients with non-metastatic colorectal cancer were analyzed for the expression of both *VEGFC* and *VEGFR3* as a function of the tumor stage. As shown in Fig. 1A and B, both *VEGFC* and *VEGFR3* were upregulated in mucosal extracts of patients with colorectal cancer, when compared with healthy control tissues, while the other lymphangiogenic growth factor *VEGFD* showed levels comparable with healthy colon tissue (Supplementary Fig. S1A). This was confirmed at the protein level on tumoral and healthy mucosal biopsies (Fig. 1C and D; Supplementary Fig. S1B), indicating that the VEGFC/VEGFR3 pathway is upregulated already at early stages of colorectal cancer progression.

Considering VEGFR3 signaling as the major inducer of lymphangiogenesis, we quantified the number of LVs in human nonmetastatic colorectal cancer and healthy tissues by IHC staining for the LV marker podoplanin. LVs were significantly increased in tumor tissues, in comparison with healthy counterparts (Fig. 1E); moreover, we confirmed not only the presence of VEGFR3 on human LVs (Fig. 1F) but also its significant overexpression on colorectal cancer–associated LECs in comparison with LECs from healthy tissues (Fig. 1G and H). As expected, the percentage of $VEGFR3^+$ LECs from healthy and colorectal cancer tissues was comparable (Fig. 1I), because most of LECs express VEGFR3.

Downloaded from cancerres.aacrjournals.org on February 26, 2020. © 2019 American Association for Cancer Research.

Published OnlineFirst June 25, 2019; DOI: 10.1158/0008-5472.CAN-18-3657

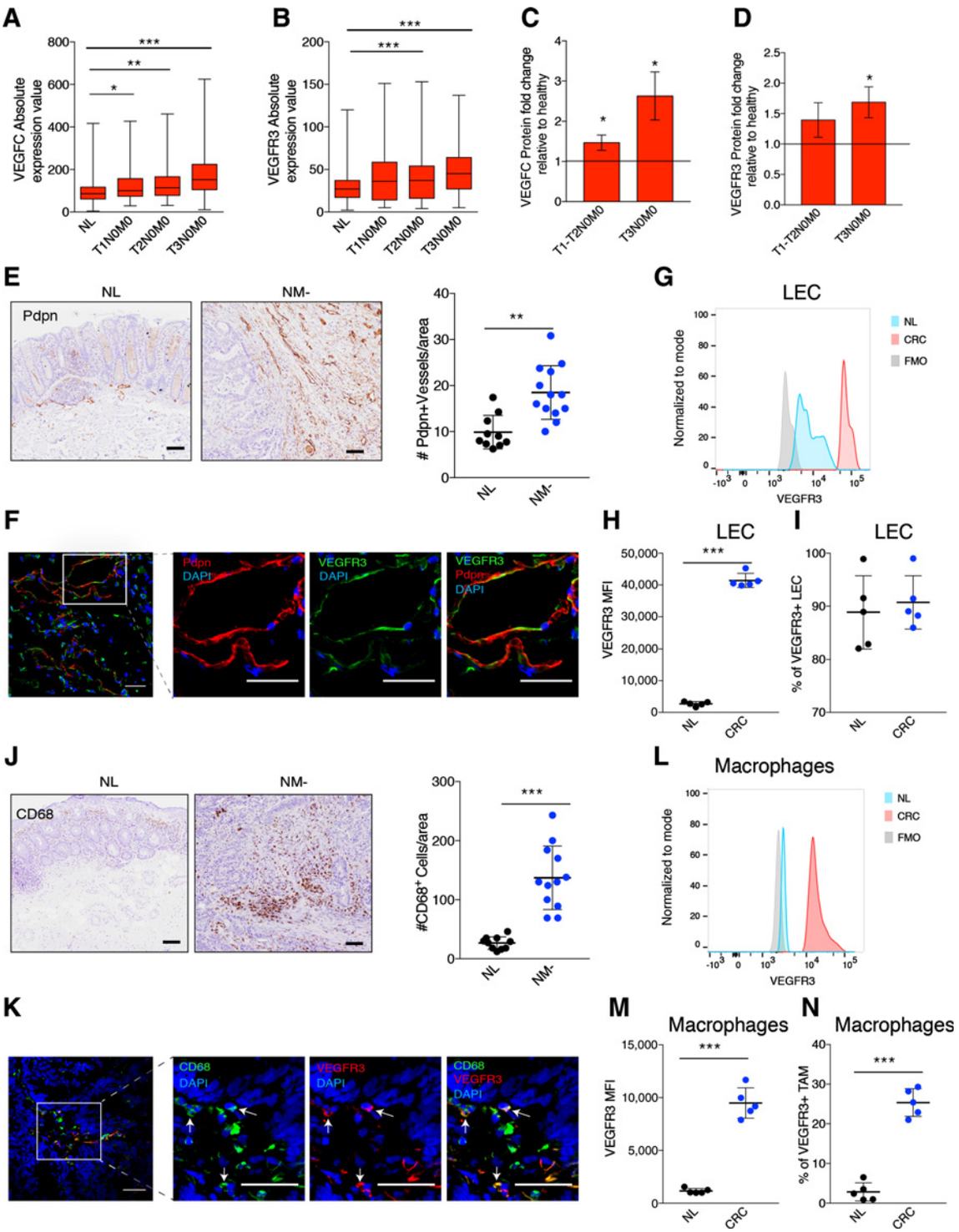

Figure 1.

The VEGFC/VEGFR3 pathway is upregulated in nonmetastatic colorectal cancer. **A** and **B,** The gene expression of *VEGFC* (**A**) and *VEGFR3* (**B**) of patients with colorectal cancer annotated in the GENT database expressed as absolute expression number and plotted according to tumor stage as median values with interquartile range (box) and range (whiskers; NL, $n = 308$; T1N0M0, $n = 36$; T2N0M0, $n = 91$; T3N0M0 $n = 131$). **C** and **D,** Western blot analysis for VEGFC (**C**) and VEGFR3 (**D**) in nonmetastatic colorectal cancer patient biopsies (NL, $n = 12$; T1-T2N0M0, $n = 6$; T3N0M0, $n = 6$). **E,** Immunostaining for Pdpn of healthy (NL, $n = 10$) and nonmetastatic (NM-, $n = 12$) colorectal cancer tissues (left) and relative quantification of $Pdpn^+$ LVs/field (right). (*Continued on the following page.*)

Downloaded from cancerres.aacrjournals.org on February 26, 2020. © 2019 American Association for Cancer Research.

Published OnlineFirst June 25, 2019; DOI: 10.1158/0008-5472.CAN-18-3657

Because we previously demonstrated that VEGFC is chemotactic for macrophages (12), we quantified TAM density in human healthy mucosa and nonmetastatic colorectal cancer tissues by IHC staining for the macrophage marker CD68. Results showed that, besides LVs, also macrophages were significantly increased in cancer tissues compared with healthy controls (Fig. 1J). Beside, similar to LVs, we found VEGFR3 to be expressed on human colorectal cancer–associated macrophages (Fig. 1K) and to be significantly increased in intensity and number on sorted TAM in comparison with macrophages from healthy colons (Fig. 1L–N), confirming a putative role for this receptor during colorectal cancer growth also in this cell type. Notably, as for human colorectal cancer, also in the azoxymethane (AOM) dextran sulphate sodium salt (DSS) nonmetastatic mouse model of colorectal cancer, *Vegfc* and *Vegfr3* levels were upregulated (Supplementary Fig. S1C) and both LV (Supplementary Fig. S1D) and TAM density (Supplementary Fig. S1E) were significantly increased in the colon of tumor-bearing mice.

Notably, we confirmed not only the presence of VEGFR3 on murine colorectal cancer–associated LVs and TAMs (Supplementary Fig. S1F–S1H), but also its upregulation by FACS in both murine LECs (Supplementary Fig. S1I) and TAMs (Supplementary Fig. S1J). Because VEGFR3 could also be expressed by blood vessels during tumor angiogenesis we analyzed by FACS the expression of VEGFR3 on $CD31^+Pdpn^-$ cells. Blood endothelial cells were found negative for VEGFR3 both in human (Supplementary Fig. S1K) and mouse tissues (Supplementary Fig. S1L). Collectively, these data demonstrate that the VEGFC/VEGFR3 pathway is upregulated in both human and murine nonmetastatic colorectal cancer and that this positively correlates with active lymphangiogenesis and TAM abundance.

Manipulation of the VEGFC/VEGFR3 pathway affects tumor growth in experimental colorectal cancer

The elevated levels of both VEGFC and VEGFR3 in nonmetastatic colorectal cancer (see Fig. 1), led us to hypothesize that these molecules might be involved in colorectal cancer development already at early stages. To investigate this hypothesis, we studied tumor response to systemic administration of VEGFC or to VEGFR3 blockade in the AOM+DSS mouse model of colorectal cancer. AOM+DSS–treated mice were administered with either an adenovirus overexpressing human VEGFC (AdVEGFC), or a VEGFR3-blocking antibody (mF431C1), while control mice received empty adenoviruses (AdGFP) or isotype-matched IgGs, according to the scheme in Supplementary Fig. S2A. VEGFC presence and VEGFR3 blockade were confirmed by Western blot at different time points (Supplementary Fig. S2B). Because DSS induces colon inflammation, clinical parameters of colitis were evaluated during the entire experiment, whereas tumor growth was quantified by colonoscopy at the termination end point. VEGFC-administered mice displayed increased tumor density (Fig. 2A and B) and size (Fig. 2A and C), while VEGFR3 blockade significantly reduced tumor number and growth compared with controls (Fig. 2A–C). Notably, neither systemic delivery of VEGFC nor VEGFR3 inhibition influenced inflammation during the entire experiment, in terms of DAI (Supplementary Fig. S2C, left), bodyweight loss (Supplementary Fig. S2C, right), and histologic inflammatory score (Supplementary Fig. S2D), suggesting that differences in tumor development and growth were not due to colitis. Surprisingly, histologic features of tumoral lesions defined as carcinomas, high-grade adenomas, low-grade adenomas, and gastrointestinal intraepithelial neoplasia, were not significantly different, indicating that tumor grading was not related to VEGFC/VEGFR3 pathway modulation (Supplementary Fig. S2E). To understand whether the effects of VEGFC were mediated exclusively by VEGFR3, we combined AdVEGFC delivery with mF431C1 treatment. Results confirmed that VEGFC acts exclusively through VEGFR3 (Supplementary Fig. S2F). In fact, mice treated with both mF431C1 and AdVEGFC (AdVEGFC+mF431C1) or adenoviral control (AdGFP+mF431C1) had similar tumor numbers and size, which were significantly reduced compared with AdGFP+IgG control group (Supplementary Fig. S2F). We next evaluated the tumor response to systemic administration of VEGFC or to VEGFR3 blockade in a second experimental model of colorectal cancer. CT26 colorectal cancer cells were orthotopically injected in the rectal mucosa of syngeneic immunocompetent animals according to the scheme in Fig. 2D. As for the AOM+DSS model, human VEGFC was enriched in the colon of AdVEGFC-treated mice (Supplementary Fig. S2G, left), while VEGFR3 activation was blocked by mF431C1 (Supplementary Fig. S2G, right). Mice treated with VEGFC showed enhanced tumor growth, while VEGFR3 blockade resulted in reduced tumor size (Fig. 2E; Supplementary Fig. S2H and S2I); as in the spontaneous model of colorectal cancer, VEGFC significantly induced tumor growth in a VEGFR3-dependent manner (Supplementary Fig. S2J), confirming the VEGFC/VEGFR3 pathway as an active promoter of colorectal cancer development, independently of experimental intestinal inflammation.

The VEGFC/VEGFR3 pathway induces lymphangiogenesis and macrophage recruitment in experimental models of colorectal cancer

Given the well-established role of the VEGFC/VEGFR3 pathway as an inducer of LV sprouting and dilation, we evaluated the effect of its manipulation in AOM+DSS–treated mice by IHC staining for LYVE-1. Results showed that while systemic blocking of

(*Continued.*) **F,** Representative immunofluorescence images of cross-sections from human nonmetastatic colorectal cancer ($n = 5$) stained for VEGFR3 (green), Pdpn (red), and DAPI (blue). **G–I,** FACS staining for VEGFR3 on cells isolated from human healthy and colorectal cancer colon tissues ($n = 5$); $VEGFR3^+$ cells were gated on living, $CD45^-$, $CD31^+Pdpn^+$ cells. VEGFR3 mean fluorescent intensity (MFI; **G**) was quantified in **H**, whereas the percentage of $VEGFR3^+$ cells is shown in **I**. **J**, Immunostaining for CD68 of healthy (NL, $n = 10$) and nonmetastatic (NM-, $n = 12$) colorectal cancer tissues (left) and relative quantification of $CD68^+$ cells/field (right). **K,** Representative immunofluorescence images of cross-sections from human nonmetastatic human colorectal cancer ($n = 5$) stained for VEGFR3 (red), CD68 (green), and DAPI (blue). **L–N,** FACS staining for VEGFR3 on cells isolated from human healthy and colorectal cancer colon tissues ($n = 5$); $VEGFR3^+$ cells were gated on living, $CD45^+$, $CD16^+CD14^+CD11b^+$ cells. VEGFR3 intensity (**L**) in the different groups was quantified in **M** and the percentage of $VEGFR3^+$ cells is shown in **N**. All data are expressed as mean ± SD. Statistical significance was determined by one-way ANOVA test with Bonferroni correction for multiple comparisons (**A–D**), unpaired Student *t* test (**E**, **H**, **I**, **J**, **M**, and **N**). Asterisks indicate statistical significance. *, $P < 0.05$;**, $P < 0.01$; ***, $P < 0.001$. Scale bars, 100 μm (**E** and **J**) and 50 μm (**F** and **K**).

Downloaded from cancerres.aacrjournals.org on February 26, 2020. © 2019 American Association for Cancer Research.

Published OnlineFirst June 25, 2019; DOI: 10.1158/0008-5472.CAN-18-3657

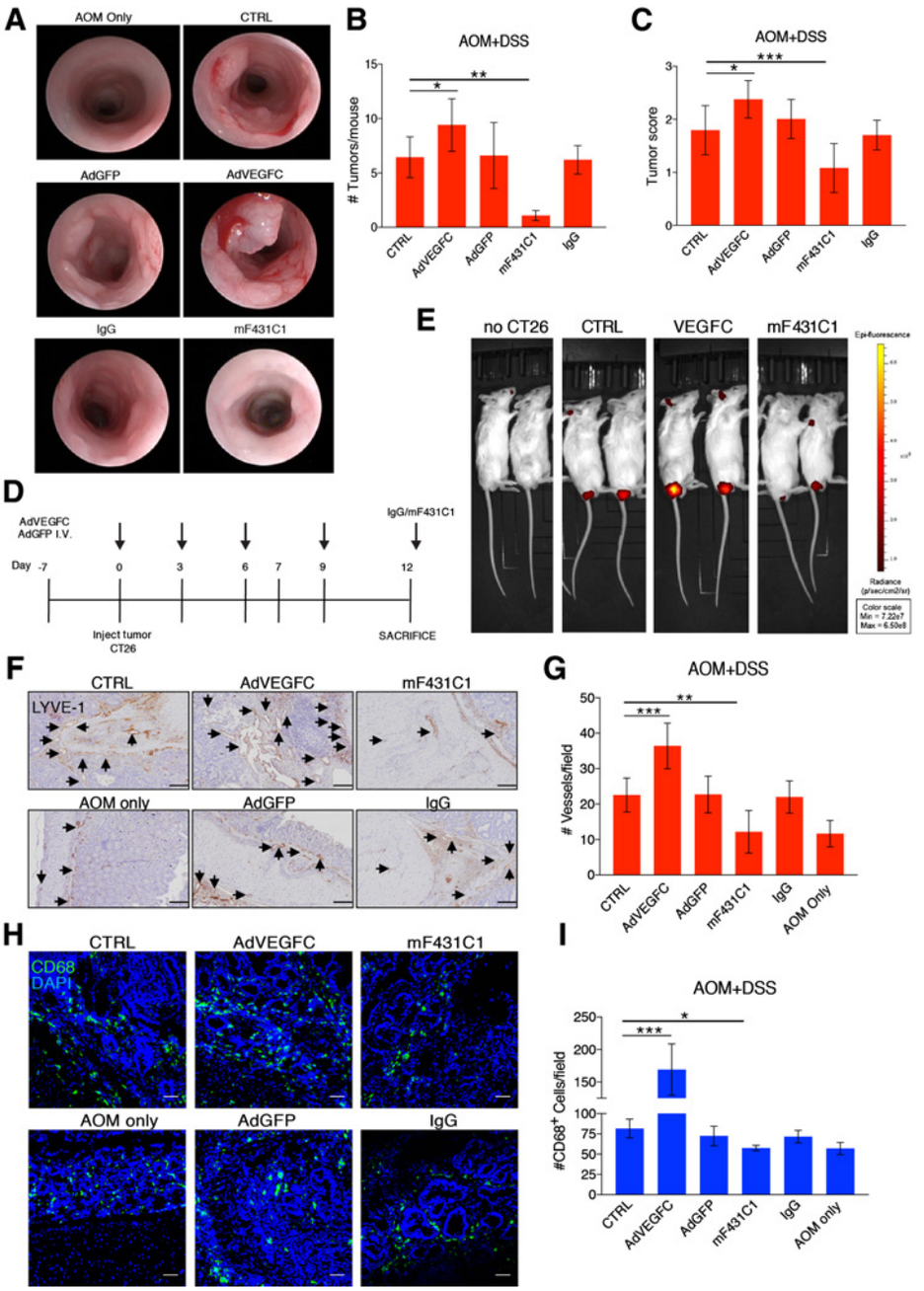

Figure. 2.

The modulation of the VEGFC/VEGFR3 pathway affects experimental colorectal cancer development. **A–C,** Mice subjected to AOM+DSS treatment were injected with AdVEGFC, or anti-VEGFR3 antibody (mF431C1), with control mice receiving empty adenoviruses (AdGFP) or isotype-matched IgGs. Representative endoscopic images showing mouse polyps at day 50 are shown in **A**. Tumor density (**B**) and size (**C**) assessed within the first 4 cm of colon from rectum to the proximal part at day 50 by endoscopic scoring ($n \geq 5$ mice/group for two independent experiments). **D,** Schematic experimental representation of CT26 orthotopic colorectal cancer model with relative treatments. **E,** mCherry-positive CT26 colorectal cancer tumor–bearing mice treated with AdVEGFC or mF431C1. Representative IVIS *in vivo* imaging pictures. Mice not injected with CT26 tumor cells (no CT26) were used as negative control. Immunostaining for LYVE-1 and CD68 of colon tissues from AOM+DSS mice with the indicated treatments (**F** and **H**) and relative quantification of LYVE-1–positive vessels (**G**) and $CD68^+$ cells (**I**) per field ($n = 5$ mice/group, with 5 fields for two independent experiments). Scale bar, 100 μm (**F**) and 50 μm (**H**). In **F,** black arrowheads indicate LYVE-1–positive LVs. All data are expressed as mean values ± SD. Statistical significance was determined by one-way ANOVA test with Dunnett correction for multiple comparisons. Asterisks indicate statistical significance. *, $P < 0.05$; **, $P < 0.01$; ***, $P < 0.001$.

VEGFR3 significantly reduced LV density in tumoral and peritumoral regions, lymphangiogenesis was enhanced by VEGFC administration (Fig. 2F and G). To quantify LV size, we performed whole-mount stainings for LYVE-1 and the pan-endothelial marker CD31 on colons of tumor-bearing mice after different treatments (Supplementary Fig. S3A). Results showed that while systemic delivery of VEGFC increased vessel dimension, treatment with mF431C1 significantly reduced LV diameters in the colon (Supplementary Fig. S3B). Furthermore, neither systemic inhibition of VEGFR3 nor delivery of VEGFC affected the number of $CD31^+$ LYVE-1- blood vessels in the colon of AOM+DSS–treated mice (Supplementary Fig. S3C and S3D), confirming that this pathway had no influence on angiogenesis in experimental colorectal cancer.

We next assessed TAM abundance in tumoral areas of AOM+DSS–treated (Fig. 2H and I) and in CT26 tumor–bearing mice (Supplementary Fig. S3E). Animals receiving VEGFC displayed increased TAM density in both tumor models; on the contrary, treatment with mF431C1 resulted in significantly reduced $CD68^+$ cells/field, compared with controls (Fig. 2I; Supplementary Fig. S3E). Importantly, we found $VEGFR3^+$ TAMs to be significantly enriched in VEGFC-treated mice, and reduced upon VEGFR3 blockade (Supplementary Fig. S3F). As revealed by IHC staining, $VEGFR3^+$ cells localizing at the tumor site were

Downloaded from cancerres.aacrjournals.org on February 26, 2020. © 2019 American Association for Cancer Research.

Published OnlineFirst June 25, 2019; DOI: 10.1158/0008-5472.CAN-18-3657

more abundant in VEGFC-treated animals (Supplementary Fig. S3G), but diminished in number in mice receiving mF431C1. Altogether, these findings highlight the involvement of VEGRF3 signaling not only in tumor lymphangiogenesis but also in the accumulation of TAMs.

VEGFR3 blockade enhances the efficacy of vaccine-induced antitumor immunity in experimental colorectal cancer

To address the potential roles of the VEGFC/VEGFR3 pathway in modulating host antitumor immunity, we evaluated T-cell density in the colon of AOM+DSS–treated mice, by IHC staining for CD3. Mice receiving VEGFC had fewer peritumoral $CD3^+$ cells, whereas animals treated with mF431C1 displayed more T lymphocytes per area, compared with controls (Fig. 3A and B).

To corroborate our hypothesis that VEGFR3 signaling could shape adaptive immune response, we stably overexpressed, by lentiviral infection, chicken ovalbumin (OVA) peptide in CT26 and MC38 adenocarcinoma cells. OVA-expressing colorectal cancer cells were next injected in the rectal mucosa of syngeneic immunocompetent mice. To test whether VEGFR3 signaling modulates preexisting antigen-specific immunity, VEGFC- and mF431C1-treated mice were vaccinated with OVA starting 14 days prior to tumor implantation and lipopolysaccharide (LPS) was used as a vaccination adjuvant (Fig. 3C). As expected, the vaccination strongly inhibited the growth of OVA-CT26 tumors (Fig. 3D). However, VEGFC administration completely abolished the effects of OVA vaccination on tumor growth (Fig. 3D); in sharp contrast, VEGFR3 inhibition in vaccinated mice resulted in massive reduction of tumor size, which was significantly smaller than in control vaccinated mice (Fig. 3D). To clarify whether systemic or local administration of VEGFC was required for suppression of the adaptive immune response, we injected OVA-overexpressing cells into the rectal mucosa of C57/Blc6 mice (Supplementary Fig. S4A). MC38 cells expressed and produced high levels of VEGFC (Supplementary Fig. S4B and S4C); however, as for CT26, MC38 did not express VEGFR3 or VEGFR2 (Supplementary Fig. S4B), indicating that these tumor cell lines cannot be directly influenced by mF431C1. Similar to AdVEGFC-administered mice, OVA-immunized or naïve mice transplanted with OVA-overexpressing MC38 cells showed comparable tumor growth (Fig. 3E–G). The inefficacy of vaccine-induced immunity was abolished by VEGFR3 blockade; in fact, mice treated with mF431C1, were more susceptible to OVA vaccination, in comparison with vaccinated animals treated with control IgGs (Fig. 3E–G). As a confirmation, vaccinated mice showed increased infiltration in the tumor of OVA (pentamer)-specific $CD8^+$ T cells upon VEGFR3 blockade (Supplementary Fig. S4D). Importantly, VEGFR3 inhibition reduced tumoral LV (Supplementary Fig. S4E and S4F) and TAM density (Supplementary Fig. S4E and S4G), while no effects were observed on blood vessels (Supplementary Fig. S4E and S4H). These findings indicate that also local VEGFC/VEGFR3 can induce antigen-specific immunotolerance, thus demonstrating a direct effect of the pathway on colorectal cancer immune-escape. We next asked if besides differences in T-cell abundance, their maturation and activation were also affected by VEGFR3 signaling (Supplementary Fig. S5A). Surprisingly, besides differences in the number of total CD8 (Fig. 3H) and CD4 (Supplementary Fig. S5B) T cells, we could not detect any difference between the groups in the percentages of CD69-activated, central memory, effector, or naïve T cells (Fig 3H; Supplementary Fig. S5A and S5B) and CD4 T regulatory cells (Supplementary Fig. S5A and S5C). Altogether, these data suggest that the VEGFC/VEGFR3 pathway can influence antitumor immunity by inhibiting T-cell proliferation rather than T-cell maturation.

Activation of VEGFR3 signaling induces macrophage polarization into immunosuppressive cells

Having confirmed that TAM abundance was affected by the VEGFC/VEGFR3 signaling, we next asked whether this pathway was also able to control macrophage activation and polarization in experimental colorectal cancer. To understand how the VEGFC/VEGFR3 pathway shapes nonmetastatic colorectal cancer–associated macrophages to promote cancer immune escape, we studied the effects of VEGFR3 blockade on the transcriptome of TAMs by RNA sequencing (RNA-seq) analysis. For this purpose, we used FACS sorting to isolate LECs and TAMs from MC38 orthotopic tumors treated with mF431C1 or control IgG (Supplementary Fig. S6A). The analysis of cell type–specific genes confirmed the purity of TAMs (Fig. 4A). RNA-seq analysis revealed that gene expression of TAMs is affected by mF431C1, as evidenced by MA plots (Fig. 4B). To confirm the reliability of RNA-seq data, we selected 2 TAM-associated genes upregulated in mF431C1-treated mice, namely BMP4 and TANK (Fig. 4C), and verified their protein expression in the AOM+DSS model under the same treatments. Both BMP4 and TANK were found significantly increased by FACS analysis in mF431C1-treated animals also in this experimental setting (Fig. 4D; Supplementary Fig. S6B). Functional annotation of the differentially modulated biological processes by gene set enrichment analysis (GSEA) showed that VEGFR3 inhibition strongly affected TAM biological functions (Fig. 4E). In fact, TAMs isolated from mF431C1-treated animals displayed differential expression of genes involved in antigen processing and presentation on MHCI, innate immune response, T-cell migration and response to IL6, and a significant downregulation of genes belonging to pathways related to cell migration, cell–cell adhesion, Toll-like receptor 4, and nitric oxide–mediated signal transduction (Fig. 4E). Accordingly, this pathway was also able to control macrophage activation and polarization in the colon of AOM+DSS–treated mice. Results showed that VEGFC administration significantly upregulated arginase, CCL2, iNOS, and FIZZ (Fig. 4F), which are known to be expressed by protumorigenic M2-like TAMs (19). On the contrary, VEGFR3 blockade resulted in a significant increase of inflammatory mediators, such as IL1β, TNFα, and CXCL10 (Fig. 4F), associated to the M1-like TAM phenotype (19). Other cytokines associated with macrophage polarization, such as IL12B, CXCL9, IL4, IL23, CCL22, and IL10, were not differentially expressed upon administration of VEGFC or mF431C1 (Supplementary Fig. S6C). This cytokine expression profile associated to TAMs was confirmed also in murine macrophages sorted from MC38 tumors (Supplementary Fig. S6D). Because we previously demonstrated that VEGFR3 signaling drives macrophage polarization toward a M2-like phenotype (12), and that this macrophage subpopulation is known to induce immunosuppression in cancer (19), we next verified whether the VEGFC/VEGFR3 pathway could be responsible for macrophage conversion into immunosuppressive cells. For this purpose, bone marrow–derived macrophages (BMDM) were stimulated *in vitro* with VEGFC- and/or SAR131675- (SAR), a VEGFR3 tyrosine kinase inhibitor, and then cocultured with splenocytes, previously labeled with CFSE (Fig. 4G). LPS+IFNγ- and IL4-stimulated BMDMs were used as controls of the

Downloaded from cancerres.aacrjournals.org on February 26, 2020. © 2019 American Association for Cancer Research.

Published OnlineFirst June 25, 2019; DOI: 10.1158/0008-5472.CAN-18-3657

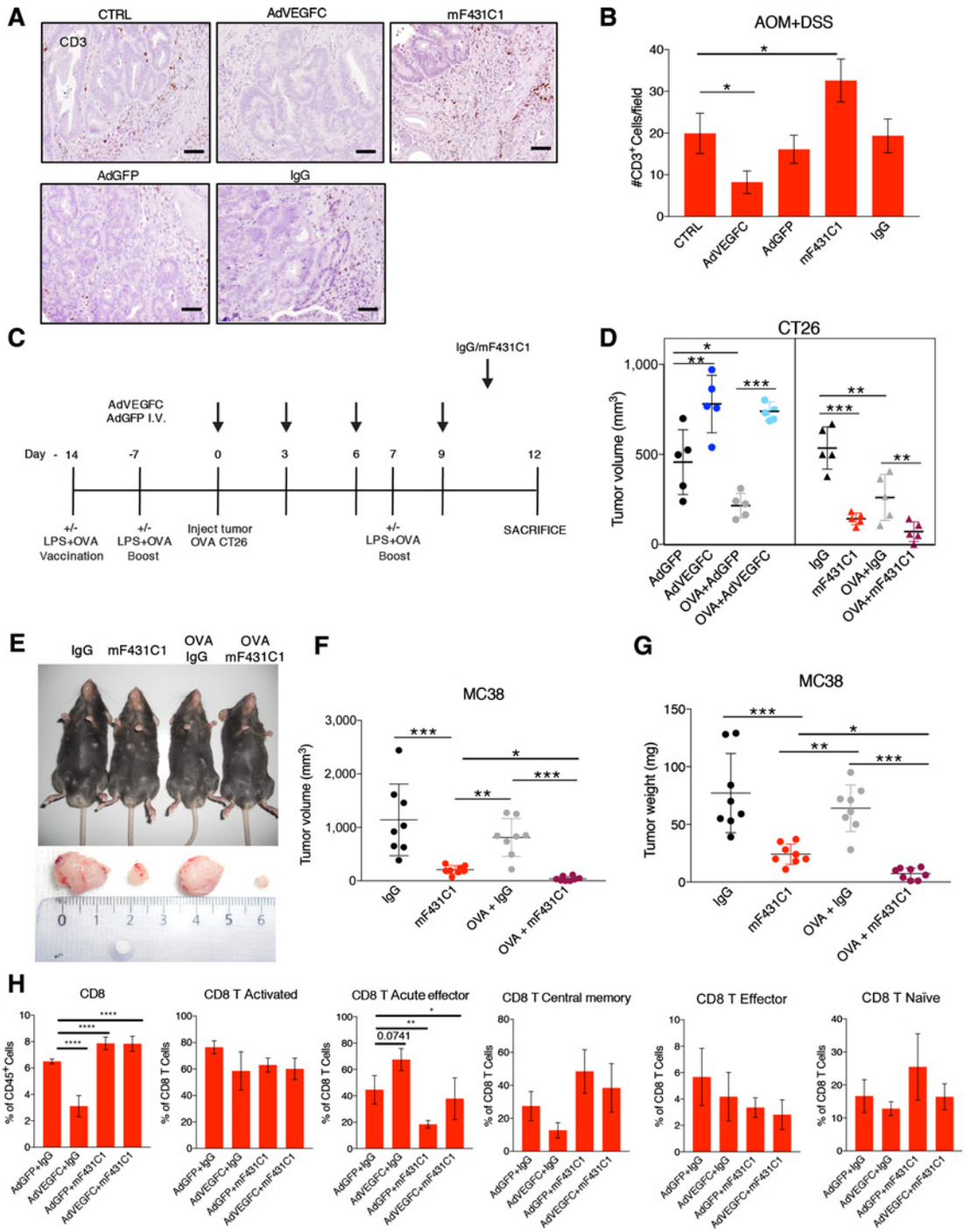

Figure 3.

Systemic and local VEGFC induce immunosuppression in experimental colorectal cancer. **A** and **B,** Representative IHC images of colonic sections from AOM+DSS mice with the indicated treatments, stained for CD3 (**A**), and relative quantification (**B**; $n \geq 4$/group of two independent experiments). Scale bar, 50 μm. **C,** OVA vaccination scheme with LPS adjuvant, AdVEGFC/AdGFP, and mF431C1/IgG in CT26 orthotopic colorectal cancer model. **D,** Tumor volume quantification of mice orthotopically injected in the rectal mucosa with OVA-overexpressing CT26 cells with the indicated treatments at day 12 ($n = 5$/group of two independent experiments). Representative pictures of MC38 tumor–bearing mice with the indicated treatments at day 14 (**E**), and relative measurement of tumor volume (**F**) and weight (**G**; $n = 8$/group representative of two independent experiments). **H,** FACS analysis of CD8 T-cell subpopulations in the CT26 tumor-bearing mice at the indicated treatments and is displayed as percentage of all $CD45^+$ cells or CD8 T cells. All data are expressed as mean values ± SD. Statistical significance was determined by one-way ANOVA test with Dunnett (**B** and **H**) or Tukey (**D**, **F**, and **G**) correction for multiple comparisons. Asterisks indicate statistical significance. *, $P < 0.05$;**, $P < 0.01$; ***, $P < 0.001$.

Downloaded from cancerres.aacrjournals.org on February 26, 2020. © 2019 American Association for Cancer Research.

Published OnlineFirst June 25, 2019; DOI: 10.1158/0008-5472.CAN-18-3657

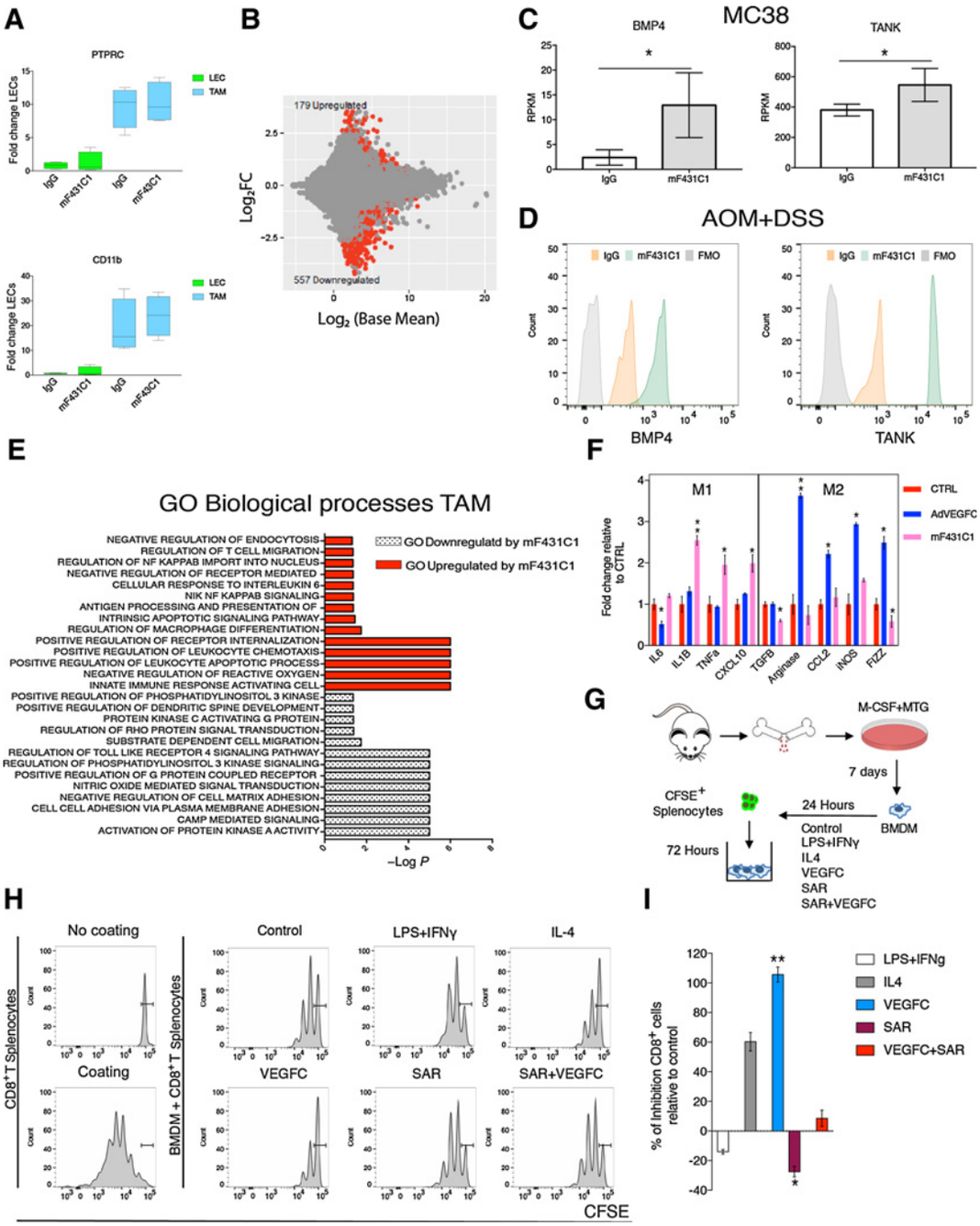

Figure 4.

The VEGFC/VEGFR3 pathway affects macrophage immune tolerance. **A–C,** RNA-seq analysis of TAMs sorted from MC38 tumors treated with mF431C1 or with IgG control. **A,** Display RNA-seq analysis of gene transcripts of interest in TAMs and LECs ($n = 4$). **B,** MA plots of differentially expressed genes identified in TAMs upon VEGFR3 inhibition. Data represent individual gene responses plotted as $\log_2$-fold change (FC) versus $\log_2$ (Base Mean). Red dots, genes differentially regulated with $P < 0.05$. **C,** BMP4 and TANK gene expression in TAMs sorted as described in **A**. **D,** FACS analysis of BMP4 and TANK mean fluorescence intensity in macrophages from AOM+DSS–treated mice administered with mF431C1 and IgG control ($n \geq 4$). **E,** Biological processes analysis of all differentially expressed genes in MC38 tumor–derived TAMs. **F,** Colonic expression of macrophage-associated genes examined by qPCR at the indicated treatments ($n \geq 4$). **G,** Schematic representation of T-cell proliferation assay after coculture with BMDMs. **H** and **I,** BMDMs, polarized with IFNγ+LPS, IL4, VEGFC, SAR, VEGFC+SAR, or medium alone (control), were cocultured with CFSE-labeled splenocytes in the presence of CD3/CD28 coating. After 72 hours, CFSE fluorescence was assessed by FACS on $CD8^+$-gated cells. Representative histograms of $CD8^+$ T with percentages of gated cells (**H**) and quantification of $CD8^+$ T-cell proliferation expressed as percentage of inhibition versus control (**I**; pooled data from three independent experiments, $n = 3$/group). All data are expressed as mean values ± SEM. Statistical significance was determined by one-way ANOVA test with Dunnett (**B**) correction for multiple comparisons and by unpaired Student *t* test (**C**, **F**, and **I**). Asterisks indicate statistical significance. *, $P < 0.05$; **, $P < 0.01$.

Downloaded from cancerres.aacrjournals.org on February 26, 2020. © 2019 American Association for Cancer Research.

Published OnlineFirst June 25, 2019; DOI: 10.1158/0008-5472.CAN-18-3657

M1/immunostimulatory or M2/immunosuppressive phenotype, respectively. After 72 hours of coculture, T-cell proliferation was evaluated gating live cells on $CD8^-$ and $CD4^+$ sub populations. As expected, pretreatment of BMDMs with LPS and IFNγ significantly increased both $CD8^+$ and $CD4^+$ T cells' proliferation, by comparison with unstimulated BMDMs (Fig. 4H and I; Supplementary Fig. S6E and S6F). VEGFC-stimulated macrophages were found to suppress both $CD8^+$ (Fig. 4H and I) and $CD4^+$ (Supplementary Fig. S6E and S6F) T cells' proliferation, in comparison with unstimulated BMDMs; these immunosuppressive effects were abolished by VEGFR3 inhibition, indicating that VEGFC-induced VEGFR3 signaling directly mediates the suppressive ability of macrophages *in vitro*. Importantly, treatment with SAR alone induced proliferation of both T-cell subpopulations, indicating that inhibition of VEGFR3 *per se* is sufficient to induce an immune-active phenotype.

Lymphatic vessels and TAMs synergistically cooperate to induce colorectal cancer growth upon VEGFR3 activation

Besides TAMs, also LVs are known to shape antitumor immunity (4–6, 16), therefore we investigated whether VEGFR3 signaling could help inducing an immune-tolerant cancer environment taking advantage of RNA-seq. Similarly to TAMs, LECs isolated from mF431C1- and IgG-treated tumors showed high purity for specific markers (Fig. 5A). Moreover, LECs derived from mF431C1-treated tumors displayed upregulation of 301 genes and downregulation of 140 genes in comparison with IgG controls (Fig. 5B), with an enrichment in processes related to inflammation, lymphocyte chemotaxis, response to ILs and IL6 secretion, and a downregulation in pathways associated with adaptive immunity (Fig. 5C). As for TAMs, we selected 2 LEC-expressing genes upregulated by mF431C1, namely TICAM1 and PVR (Fig. 5D), and found the relative proteins to be significantly increased also in LECs from the AOM+DSS model under the same treatments (Fig. 5E; Supplementary Fig. S7A). To elucidate whether the VEGFC/VEGFR3 pathway can induce immunosuppression directly through LECs, we performed a coculture experiment with human intestinal LECs pretreated with VEGFC and/or SAR, and blood-derived T cells (Fig. 5F). Interestingly, VEGFC-treated HILECs significantly inhibited CD8 T (Fig. 5G and H) and, to lesser extent, CD4 T cells (Supplementary Fig. S7B and S7C) in a VEGFR3-dependent manner. Of note, SAR alone was able to induce T-cell proliferation mainly of CD8 T cells (Fig. 5G and H). These data suggest that upon VEGFR3 blockade, intestinal LECs may lose their protolerogenic properties (4), thus granting a proper antitumoral immune response.

Our data indicate that both LVs and TAMs are affected by the modulation of the VEGFC/VEGFR3 pathway and that both cell types could potentially contribute to colorectal cancer development (5, 13, 15, 20). To elucidate which cell compartment among LVs and TAMs is responsible for the enhanced tumor growth observed in response to VEGFR3 signaling, we depleted macrophages in the CT26 orthotopic colorectal cancer model using BLZ945 (BLZ), a small molecule that blocks colony-stimulating factor receptor (CSF1R; ref. 21), according to the scheme in Fig. 6A. Mice treated with BLZ or vehicle were further administered with AdVEGFC and/or mF431C1. Treatment with BLZ did not influence tumor growth (Fig. 6B) in comparison with vehicle-treated mice. Strikingly, protumorigenic effects exerted by VEGFC were significantly reduced upon macrophage depletion, although tumor volume was still significantly bigger than the control vehicle-treated group, confirming that TAMs are not the only contributors to colorectal cancer development (Fig. 6B). Remarkably, macrophage depletion, confirmed by FACS (Supplementary Fig. S8A) and immunofluorescence (Supplementary Fig. S8B and S8C), did not further inhibit tumor growth in mF431C1-treated animals (Fig. 6B), indicating that, apart from TAMs, also LVs play a crucial role in colorectal cancer onset. Of note, VEGFC exerted its protumorigenic effects exclusively via VEGFR3 activation; in fact, mF431C1 abolished VEGFC-induced tumor growth (Fig. 6B). Notably, depletion of TAMs did not affect LV density (Supplementary Fig. S8B and S8D) or angiogenesis (Supplementary Fig. S8B and S8E). Importantly, VEGFC reduced both $CD8^+$ and $CD4^+$ T lymphocytes, while VEGFR3 blockade resulted in enhanced recruitment of T cells at the tumor site (Fig. 6C and D; Supplementary Fig. S8F and S8G). Remarkably, $CD8^+$ and $CD4^+$ T-cell density inversely correlated not only with tumor size (Fig. 6E and F), but also with the number of TAMs (Fig. 6G and H) and LVs (Fig. 6I and J), indicating that adaptive immunity is dampened in response to activation of VEGFR3 signaling in colorectal cancer–associated LVs and macrophages. Overall, these data demonstrate that VEGFC-induced tumor growth relies on a synergistic cooperation between $VEGFR3^+$TAMs and LVs, which affects antitumor immunity in a VEGFR3-dependent manner (Fig. 7A).

To finally investigate whether mF431C1 could indeed provide therapeutic efficacy in colorectal cancer, MC38 tumors were let to establish for 1 week and mice were then randomized and administered 3 times per week with mF431C1 or IgG control (Fig. 7B). Consistent with our expectation, blockade of VEGFR3 provided therapeutic efficacy and strongly reduced the tumor volume in mF431C1-treated animals (Fig. 7C), supporting VEGFR3 blockade as an efficient therapy for nonmetastatic colorectal cancer.

Discussion

Hallmarks of cancer immunoediting are as follows: (i) the elimination of tumor cells by innate or adaptive immune system; (ii) the persistence, during which the elimination step fails, leading to a balance between proliferating cancer cells and immunosurveillance; and (iii) the escape, during which proliferating cancer cells overcome the protective effect of the immune system due to immune exhaustion/inhibition (22). In this scenario, cytokines and growth factors released in the tumor microenvironment acquire the capability not only to shape the functional orientation of immune cells, such as TAMs (8), but also to affect several biological processes, which sustain tumor growth, including angiogenesis, and lymphangiogenesis (23), thus controlling the overall balance between tumor eradication and tumor promotion.

We here found that VEGFC, a growth factor involved in cancer-associated lymphangiogenesis whose expression in human tumors strongly correlates with poor prognosis (24), is upregulated in nonmetastatic colorectal cancer, together with its cognate receptor VEGFR3, indicating a potential role for this signaling axis in colorectal cancer development. This hypothesis was corroborated by our *in vivo* studies, in which we discovered that while administration of VEGFC in mice exacerbated colorectal cancer tumorigenesis, VEGFR3 blockade had a strong antitumoral activity. These findings are in accordance with other works showing an involvement of the VEGFC/VEGFR3 pathway in early phases of tumor development (15), and are in line with studies

Downloaded from cancerres.aacrjournals.org on February 26, 2020. © 2019 American Association for Cancer Research.

Published OnlineFirst June 25, 2019; DOI: 10.1158/0008-5472.CAN-18-3657

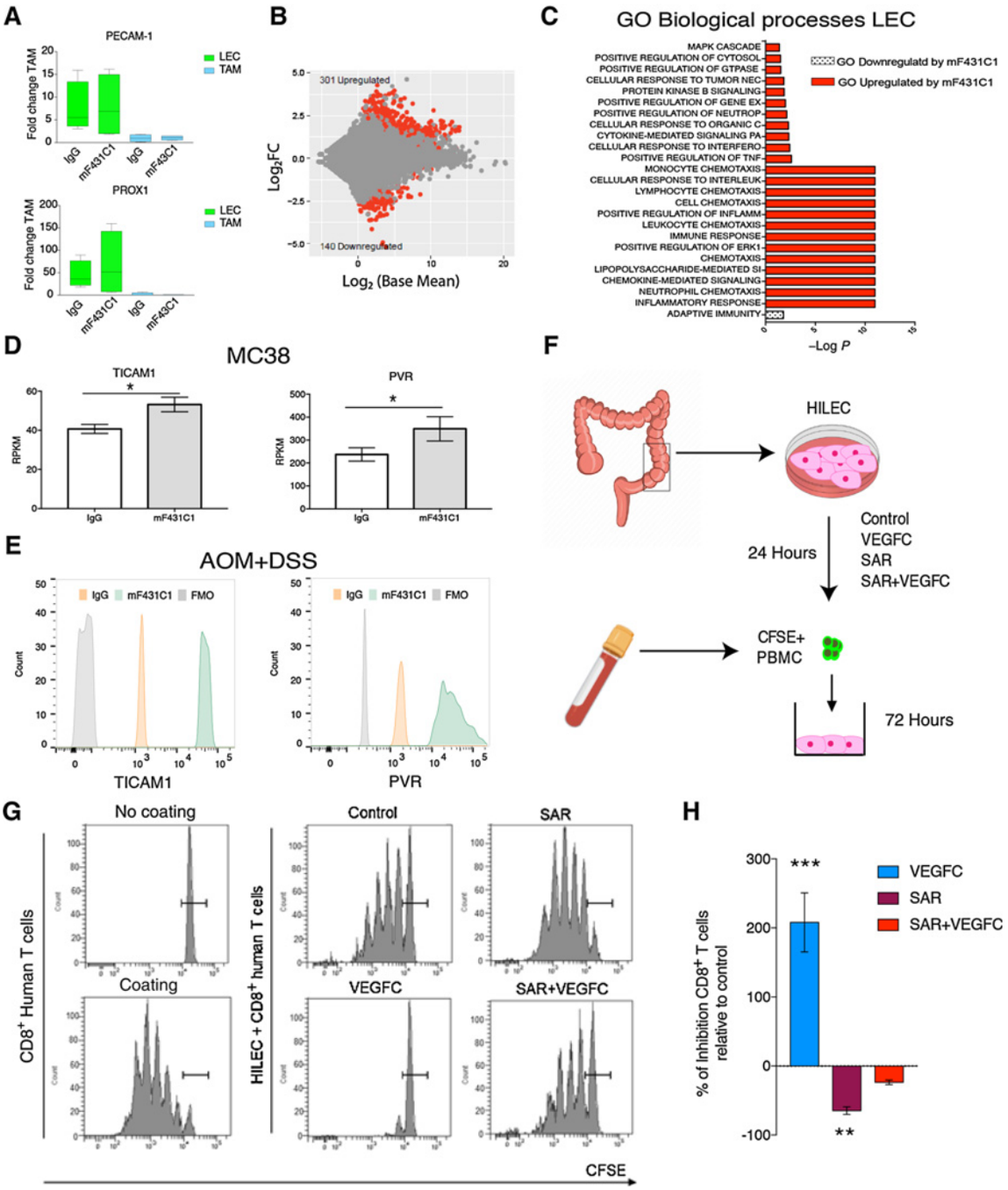

Figure 5.

The VEGFR3 signaling affects LECs immune suppression. **A–C,** RNA-seq analysis of LECs sorted from orthotopic MC38 tumor–bearing mice treated with mF431C1 or with IgG control. **A,** Displays RNA-seq analysis of gene transcripts of interest in TAMs and LECs ($n = 4$). **B,** MA plots of differentially expressed genes identified in LECs upon VEGFR3 inhibition. Data represent individual gene responses plotted as $\log_2$FC versus $\log_2$ (Base Mean). Red dots, genes differentially regulated with $P < 0.05$. **C,** shows the biological processes analysis of all differentially expressed genes in MC38 tumor–derived LECs. **D,** TICAM1 and PVR expression in LECs sorted as described in **A**. **E,** FACS analysis of TICAM1 and PVR mean fluorescence intensity in LECs from AOM+DSS–treated mice administered with mF431C1 and IgG control ($n \geq 4$). **F,** Schematic representation of T-cell proliferation assay after coculture of PBMCs with HILEC. **G** and **H,** HILECs treated with VEGFC, SAR, VEGFC+SAR, or medium alone (control) were cocultured with CFSE-labeled PBMCs in the presence of CD3/CD28 coating. After 72 hours, CFSE fluorescence was assessed by FACS on $CD8^+$T cells. **G** and **H,** Representative histograms of $CD8^+$ T-cell proliferation with percentages of gated cells (**G**) and relative bar graphs (**H**) expressed as percentage of proliferation inhibition versus control ($n = 4$). All data are expressed as mean values ± SEM. Statistical significance was determined by one-way ANOVA test with Dunnett (**B**) correction for multiple comparisons and by unpaired Student *t* test. Asterisks indicate statistical significance. *, $P < 0.05$;**, $P < 0.01$; ***, $P < 0.001$.

Downloaded from cancerres.aacrjournals.org on February 26, 2020. © 2019 American Association for Cancer Research.

Published OnlineFirst June 25, 2019; DOI: 10.1158/0008-5472.CAN-18-3657

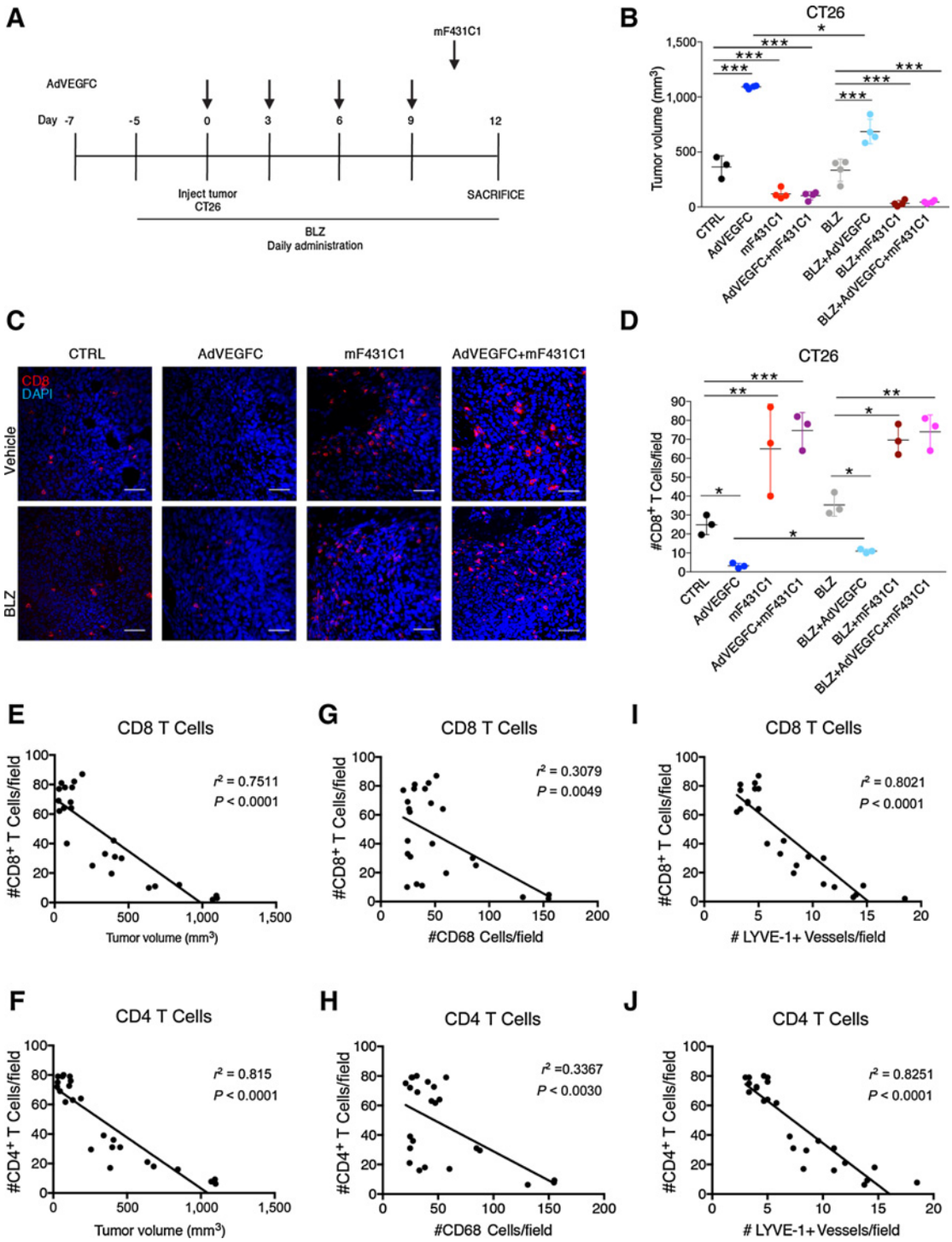

Figure 6.

The VEGFC/VEGFR3 pathway induces immune tolerance through a synergistic cooperation of lymphatic vessels and macrophages. **A,** BLZ treatment scheme with AdVEGFC and mF431C1 administration regimen CT26 colorectal cancer–bearing mice. **B,** Tumor volume quantification of CT26 tumor–bearing mice at day 12 ($n \geq 3$ representative of two independent experiments). **C,** Representative immunofluorescence images ($n = 5$ images/tumor) of cross-sections from CT26 tumor–bearing mice ($n = 3$) stained for DAPI (blue), CD8 (red), and relative quantification (**D**). Scale bar, 50 μm. **E–J,** Scatter plots showing the linear correlations between the values of $CD8^+$T or $CD4^+$ T-cell density quantified by immunofluorescence and the CT26 tumor volume measured by caliper at day 12 (**E** and **F**), TAMs (**G** and **H**), and LVs (**I** and **J**). Significance was determined by one-way ANOVA test with Tukey correction for multiple comparisons or by linear regression analysis. Asterisks indicate statistical significance. *, $P < 0.05$; **, $P < 0.01$; ***, $P < 0.001$.

Downloaded from cancerres.aacrjournals.org on February 26, 2020. © 2019 American Association for Cancer Research.

Published OnlineFirst June 25, 2019; DOI: 10.1158/0008-5472.CAN-18-3657

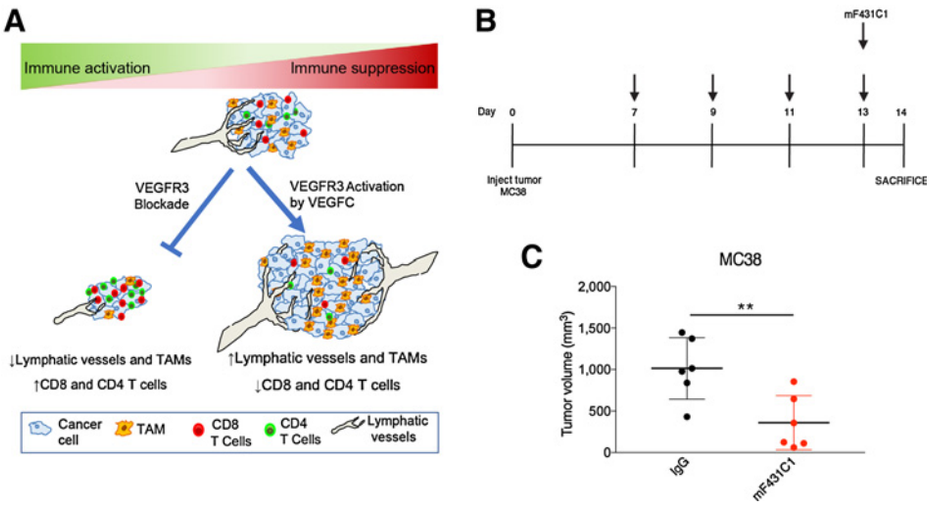

Figure 7.

Activation of the VEGFC/VEGFR3 pathway in LVs and TAMs induces tumor immune escape in colorectal cancer. **A,** VEGFC binding to VEGFR3 on LVs and TAMs (right) increases their density and function during experimental colorectal cancer development, leading to immune suppression, in terms of reduced number of $CD4^+$ and $CD8^+$ T cells. On the contrary, VEGFR3 inhibition (left) blocks both lymphangiogenesis and TAM density, along with their immunosuppressive properties, thus promoting activation of a proper antitumor immune response, in terms of increased number of $CD4^+$ and $CD8^+$ T cells. **B,** Schematic representation of therapeutic mF431C1 administration regimen in mice orthotopically injected in the rectal mucosa with MC38 cells. **C,** Tumor volume quantification of MC38 tumor—bearing mice, with the indicated treatments at day 14 by caliper ($n = 6$ mice/group). Data are expressed as mean ± SD. **, $P < 0.01$ by two-tailed unpaired Student t test.

performed on melanoma, skin, and breast cancer, which observed that VEGFR3 inhibition could attenuate tumor growth (5, 13, 15, 16, 20). Growing evidence supports a role for lymphangiogenesis in chronic inflammation (25, 26). VEGFR3 signaling has been, in fact, proposed as a promising therapeutic target in inflammatory disorders (27). Besides, several studies, including our own (25), have demonstrated beneficial effects of VEGFC delivery in animal models of chronic inflammation (27, 28). With regard to IBD, our previous study showed that inhibition of VEGFR3 lead to exacerbation of intestinal inflammation, whereas delivery of VEGFC ameliorated colitis outcome (25). Unlike our previous study (25), we could not observe significant changes in inflammatory scores of colitis in the AOM+DSS model, upon modulation of VEGFR3 signaling. These contrasting results could be due to the different inflammatory degree of the AOM+DSS model in comparison with the DSS-induced model of chronic colitis. In fact, while a mild damage of the intestinal epithelial layer previously "initiated" by the carcinogen AOM, and a moderate inflammatory milieu are the major features of the tumor model, a more severe inflammation and epithelial erosion characterize the second model; thus, we can assume that the protective effects observed with the anti-VEGFR3 antibody on tumor development are independent from experimental intestinal inflammation. This is in line with other studies reporting discrepancies between the AOM+DSS and the DSS alone–induced models. As an example, while Scaldaferri and colleagues, demonstrated that the inhibition of VEGFA has beneficial effects on colitic animals (29), Waldner and colleagues did not observe an amelioration of colitis in VEGFA-inhibited animals undergoing the AOM+DSS model of colorectal cancer (30).

An important and unique finding of our work was that VEGFR3 is expressed not only by colorectal cancer-associated LECs, but also by TAMs, and that VEGFC/VEGFR3 signaling can shape both these two cell types to synergistically inhibit antitumor immunity and promote tumor growth. In greater detail, we proved that (i) VEGFC binding to VEGFR3 modulates LV and TAM density during experimental colorectal cancer development, (ii) macrophage and LV abundance positively correlates with VEGFC-induced colorectal cancer growth, while it is reduced by VEGFR3 inhibition, and (iii) $VEGFR3^+$ LVs and TAMs control adaptive immunity, promoting colorectal cancer immune escape (Fig. 7A). This is further corroborated by our recent publication in which CT26 cells were orthotopically injected in BALB/c immunodeficient mice. The modulation of the VEGFC/VEGFR3 pathway in mice that lack T cells, resulted indeed in different micrometastasis dissemination at distant organs, but did not affect colorectal cancer primary tumor growth (2). These results together with this study's findings demonstrate that VEGFR3 signaling can modify adaptive immunity promoting colorectal cancer growth.

Even if the suppressive capacity of LECs has been previously reported in coculture experiments with T cells (31), the immunity-related effects elicited by VEGFC/VEGFR3 signaling on LECs are still in their infancy. Recently, the LVs have been found to affect immune cell function by expressing immunomodulatory molecules (32). Lund and colleagues previously showed that lymph node LECs can directly suppress antitumor T-cell responses in melanoma by tolerogenic cross-presentation of tumor antigens (5). Accordingly, our transcriptomic data on tumor-associated LECs depict the adaptive immunity-related pathway as the most prominent process modulated by VEGFR3, thus indicating a potentiated LEC immunosuppressive activity. These observations were further confirmed *in vitro* where VEGFC-stimulated HILECs inhibited T-cell proliferation in a VEGFR3-dependent manner. The fact that VEGFC promotes tumor immunosuppression (5), suggests that lymphangiogenesis inhibitors may be clinically used in combination with immunotherapy.

Downloaded from cancerres.aacrjournals.org on February 26, 2020. © 2019 American Association for Cancer Research.

Published OnlineFirst June 25, 2019; DOI: 10.1158/0008-5472.CAN-18-3657

Besides, similar effects were partially shown by other groups in both cell types and different settings. Dieterich and colleagues demonstrated that VEGFR3 activation exerts direct *in vitro* anti-inflammatory effects on LECs, by downregulation of various genes associated to immune- and cytokine-response (33). Nevertheless, Fankhauser and colleagues recently reported that VEGFR3 blockade results in reduced naïve T-cell recruitment in a mouse model of late-stage melanoma and increased VEGFC serum levels were associated with robust T-cell responses in patients with metastatic melanoma (32). This discrepancy may be explained by the fact that different tumor locations (skin vs. colon) and grade (metastatic vs. nonmetastatic) may have shaped distinct suppressive elements in the tumoral microenvironment. Interestingly, although not observed in melanoma, TAM recruitment and T-cell density were significantly affected by the modulation of VEGFR3 signaling in all our colorectal cancer mouse models, while we did not observe significant differences in T-cell maturation and subtypes, indicating a tissue-dependent effect of the VEGFC/VEGFR3 pathway.

The immunomodulatory effects exerted by VEGFR3 blockade on LECs were also observed in TAMs in which antigen processing, presentation of exogenous peptide antigen via MHC class I, and regulation of T-cell migration were among the most upregulated pathways in comparison with TAMs from IgG-administered mice. These data are in line with our coculture studies where VEGFR3 inhibition restored T-lymphocyte proliferation in the presence of VEGFC. Moreover, in the study by Zhang and colleagues, VEGFC binding to VEGFR3 inhibited the production of proinflammatory cytokines in macrophages by suppressing the TLR4-NF-κB signaling cascade during endotoxin shock (34). Consistently, we found that VEGFR3 inhibition upregulated biological processes related to NF-κB signaling and its translocation into the nucleus. Our *in vivo* experiments also showed that VEGFC-dependent activation of VEGFR3 promoted colorectal cancer through recruitment of TAMs and weakened antitumor adaptive immunity. This is in accordance with results from Espagnolle and colleagues, who demonstrated that VEGFR3 inhibition is able to modify TAM density and the ratio of M2/M1 macrophages in breast cancer (13). The differences observed in macrophage abundance upon activation of VEGFR3 signaling could be explained by a direct modulation of the NF-κB pathway in TAMs. It has been previously shown that constitutive NF-κB activation is essential for macrophage survival (35); therefore, VEGFR3 blockade could lead to reduced macrophage survival, while VEGFC might promote TAM survival through activation of NF-κB signaling. Besides a direct effect of VEGFC on macrophage survival, it was reported that LECs themselves are able to recruit macrophages in response to LPS through activation of the TLR4 pathway (36). In our experimental models of colorectal cancer, VEGFC increases peritumoral and tumoral LV density, which could then be activated by LPS extremely abundant in the gut. We thus cannot exclude that LPS-activated LECs could contribute to increased macrophage recruitment compared with tumors where lymphangiogenesis is inhibited by mF431C1. It has to be noted that, despite what has been shown by other groups, we did not observe any reduction of tumor volume and weight upon macrophage depletion with BLZ alone compared with vehicle (37, 38). These contrasting results could be due to (i) different tumor type (21); (ii) the orthotopic rather than heterotopic transplantation of colorectal cancer cells (37) and (iii) the different macrophage depletion approach (38).

As previously reported by others, we excluded a direct effect of the VEGFC/VEGFR3 pathway on the blood vasculature (39, 40) and on tumor cells, which we showed to not express VEGFR3 or to respond to VEGFC stimulation (2). However, we cannot exclude that VEGFR3 blockade or VEGFC stimulation could affect other cell types that express VEGFR3 located in other organs, such as CD11b splenic cells, myeloid suppressor cells, blood monocytes, and on nonendothelial bone marrow–derived cells (13, 41, 42).

The use of neutralizing antibodies targeting VEGFC and/or VEGFR3 in clinical studies that have progressed to phase I trials in patients with advanced solid tumors have provided encouraging results (23). Furthermore, several small-molecule protein kinase inhibitors (PKI) targeting various kinases, including VEGFR3, are now available and some of them have been approved for the treatment of colorectal cancer. For example regorafenib (43, 44), nintedanib (45), fruquintinib (46) and famitinib (47) progressed to phase II and III clinical trial, showing benefit without significant toxicity. These clinical data indicate that blocking VEGFR3 could provide a safe therapeutic approach also in nonmetastatic colorectal cancer. These clinical data together with our findings that both VEGFC and VEGFR3 levels are elevated and TAMs and LVs are increased, indicate that blocking VEGFR3 could provide a safe therapeutic approach also in nonmetastatic colorectal cancer.

In summary, our findings strongly support and encourage a VEGFC/VEGFR3–targeted therapy for blocking primary colorectal cancer tumor growth through restoration of a proper antitumor immune response. The inhibition of this signaling pathway may reduce tumor lymphangiogenesis, and protumorigenic TAMs infiltrating the tumor site, thus impeding the colorectal cancer to escape host immunity.

Disclosure of Potential Conflicts of Interest

No potential conflicts of interest were disclosed.

Authors' Contributions

Conception and design: C. Tacconi, M. Detmar, S. D'Alessio
Development of methodology: C. Tacconi, S. D'Alessio
Acquisition of data (provided animals, acquired and managed patients, provided facilities, etc.): C. Tacconi, C. Correale, A. Spinelli, A.I. Oliveira, S. Spanò, F.S. Colombo, A. Malesci, S. D'Alessio
Analysis and interpretation of data (e.g., statistical analysis, biostatistics, computational analysis): C. Tacconi, F. Ungaro, V. Arena, L. Massimino, M. Mazzone, F. Rubbino, V. Garlatti, E. Lugli, S. Danese, S. D'Alessio
Writing, review, and/or revision of the manuscript: C. Tacconi, F. Ungaro, L. Massimino, M. Detmar, M. Mazzone, A.I. Oliveira, E. Lugli, A. Malesci, L. Peyrin-Biroulet, S. Vetrano, S. Danese, S. D'Alessio
Administrative, technical, or material support (i.e., reporting or organizing data, constructing databases): C. Tacconi, C. Correale, M. Carvello,
Study supervision: C. Tacconi, M. Carvello, A. Malesci, S. D'Alessio

Acknowledgments

We thank Ron Haskell (ViraQuest Inc.) for his expert technical assistance with adenovirus preparation. Dr. Bronislaw Pytowski (Eli Lilly) provided the VEGFR3 blocking Ab mF431C1. This study was supported by grants from the Italian Ministry of Health GR-2011-02348069 to S. Danese, AIRC IG10205 to S. Danese, and PRIN 2010K34C45_003 to A. Malesci.

The costs of publication of this article were defrayed in part by the payment of page charges. This article must therefore be hereby marked *advertisement* in accordance with 18 U.S.C. Section 1734 solely to indicate this fact.

Received November 27, 2018; revised May 9, 2019; accepted June 13, 2019; published first June 25, 2019.

Downloaded from cancerres.aacrjournals.org on February 26, 2020. © 2019 American Association for Cancer Research.

Published OnlineFirst June 25, 2019; DOI: 10.1158/0008-5472.CAN-18-3657

References

1. Marmol I, Sanchez-de-Diego C, Pradilla Dieste A, Cerrada E, Rodriguez Yoldi MJ. Colorectal carcinoma: a general overview and future perspectives in colorectal cancer. Int J Mol Sci 2017;18. doi: 10.3390/ijms18010197.
2. Tacconi C, Correale C, Gandelli A, Spinelli A, Dejana E, D'Alessio S, et al. Vascular endothelial growth factor C disrupts the endothelial lymphatic barrier to promote colorectal cancer invasion. Gastroenterology 2015;148: 1438–51.
3. Liao S, Padera TP. Lymphatic function and immune regulation in health and disease. Lymphat Res Biol 2013;11:136–43.
4. Dieterich LC, Ikenberg K, Cetintas T, Kapaklikaya K, Hutmacher C, Detmar M. Tumor-associated lymphatic vessels upregulate PDL1 to inhibit T-cell activation. Front Immunol 2017;8:66.
5. Lund AW, Duraes FV, Hirosue S, Raghavan VR, Nembrini C, Thomas SN, et al. VEGF-C promotes immune tolerance in B16 melanomas and cross-presentation of tumor antigen by lymph node lymphatics. Cell Rep 2012;1: 191–9.
6. Ma Q, Dieterich LC, Detmar M. Multiple roles of lymphatic vessels in tumor progression. Curr Opin Immunol 2018;53:7–12.
7. Kang JC, Chen JS, Lee CH, Chang JJ, Shieh YS. Intratumoral macrophage counts correlate with tumor progression in colorectal cancer. J Surg Oncol 2010;102:242–8.
8. Biswas SK, Mantovani A. Macrophage plasticity and interaction with lymphocyte subsets: cancer as a paradigm. Nat Immunol 2010;11:889–96.
9. Zhao Q, Kuang DM, Wu Y, Xiao X, Li XF, Li TJ, et al. Activated $CD69^{+}$ T cells foster immune privilege by regulating IDO expression in tumor-associated macrophages. J Immunol 2012;188:1117–24.
10. Netea-Maier RT, Smit JWA, Netea MG. Metabolic changes in tumor cells and tumor-associated macrophages: a mutual relationship. Cancer Lett 2018;413:102–9.
11. Nielsen SR, Schmid MC. Macrophages as key drivers of cancer progression and metastasis. Mediators Inflamm 2017;2017:9624760.
12. D'Alessio S, Correale C, Tacconi C, Gandelli A, Pietrogrande G, Vetrano S, et al. VEGF-C-dependent stimulation of lymphatic function ameliorates experimental inflammatory bowel disease. J Clin Invest 2014;124: 3863–78.
13. Espagnolle N, Barron P, Mandron M, Blanc I, Bonnin J, Agnel M, et al. Specific inhibition of the VEGFR-3 tyrosine kinase by SAR131675 reduces peripheral and tumor associated immunosuppressive myeloid cells. Cancers 2014;6:472–90.
14. Alishekevitz D, Gingis-Velitski S, Kaidar-Person O, Gutter-Kapon L, Scherer SD, Raviv Z, et al. Macrophage-induced lymphangiogenesis and metastasis following paclitaxel chemotherapy is regulated by VEGFR3. Cell Rep 2016; 17:1344–56.
15. Alitalo AK, Proulx ST, Karaman S, Aebischer D, Martino S, Jost M, et al. VEGF-C and VEGF-D blockade inhibits inflammatory skin carcinogenesis. Cancer Res 2013;73:4212–21.
16. Lund AW, Wagner M, Fankhauser M, Steinskog ES, Broggi MA, Spranger S, et al. Lymphatic vessels regulate immune microenvironments in human and murine melanoma. J Clin Invest 2016;126:3389–402.
17. Wirtz S, Nagel G, Eshkind L, Neurath MF, Samson LD, Kaina B. Both base excision repair and O6-methylguanine-DNA methyltransferase protect against methylation-induced colon carcinogenesis. Carcinogenesis 2010; 31:2111–7.
18. Lee AY, Chang SY, Kim JI, Cha HR, Jang MH, Yamamoto M, et al. Dendritic cells in colonic patches and iliac lymph nodes are essential in mucosal IgA induction following intrarectal administration via CCR7 interaction. Eur J Immunol 2008;38:1127–37.
19. Chanmee T, Ontong P, Konno K, Itano N. Tumor-associated macrophages as major players in the tumor microenvironment. Cancers 2014;6: 1670–90.
20. Alam A, Blanc I, Gueguen-Dorbes G, Duclos O, Bonnin J, Barron P, et al. SAR131675, a potent and selective VEGFR-3-TK inhibitor with antilymphangiogenic, antitumoral, and antimetastatic activities. Mol Cancer Ther 2012;11:1637–49.
21. Pyonteck SM, Akkari L, Schuhmacher AJ, Bowman RL, Sevenich L, Quail DF, et al. CSF-1R inhibition alters macrophage polarization and blocks glioma progression. Nat Med 2013;19:1264–72.
22. Smyth MJ, Dunn GP, Schreiber RD. Cancer immunosurveillance and immunoediting: the roles of immunity in suppressing tumor development and shaping tumor immunogenicity. Adv Immunol 2006;90:1–50.
23. Stacker SA, Williams SP, Karnezis T, Shayan R, Fox SB, Achen MG. Lymphangiogenesis and lymphatic vessel remodelling in cancer. Nat Rev Cancer 2014;14:159–72.
24. Chen JC, Chang YW, Hong CC, Yu YH, Su JL. The role of the VEGF-C/VEGFRs axis in tumor progression and therapy. Int J Mol Sci 2012;14: 88–107.
25. Langner C, Harbaum L, Pollheimer MJ, Kornprat P, Lindtner RA, Schlemmer A, et al. Mucinous differentiation in colorectal cancer–indicator of poor prognosis? Histopathology 2012;60:1060–72.
26. Jurisic G, Sundberg JP, Detmar M. Blockade of VEGF receptor-3 aggravates inflammatory bowel disease and lymphatic vessel enlargement. Inflamm Bowel Dis 2013;19:1983–9.
27. Hagura A, Asai J, Maruyama K, Takenaka H, Kinoshita S, Katoh N. The VEGF-C/VEGFR3 signaling pathway contributes to resolving chronic skin inflammation by activating lymphatic vessel function. J Dermatol Sci 2014; 73:135–41.
28. Zhou Q, Guo R, Wood R, Boyce BF, Liang Q, Wang YJ, et al. Vascular endothelial growth factor C attenuates joint damage in chronic inflammatory arthritis by accelerating local lymphatic drainage in mice. Arthritis Rheum 2011;63:2318–28.
29. Scaldaferri F, Vetrano S, Sans M, Arena V, Straface G, Stigliano E, et al. VEGF-A links angiogenesis and inflammation in inflammatory bowel disease pathogenesis. Gastroenterology 2009;136:585–95.
30. Waldner MJ, Wirtz S, Jefremow A, Warntjen M, Neufert C, Atreya R, et al. VEGF receptor signaling links inflammation and tumorigenesis in colitis-associated cancer. J Exp Med 2010;207:2855–68.
31. Lukacs-Kornek V, Malhotra D, Fletcher AL, Acton SE, Elpek KG, Tayalia P, et al. Regulated release of nitric oxide by nonhematopoietic stroma controls expansion of the activated T cell pool in lymph nodes. Nat Immunol 2011;12:1096–104.
32. Fankhauser M, Broggi MAS, Potin L, Bordry N, Jeanbart L, Lund AW, et al. Tumor lymphangiogenesis promotes T cell infiltration and potentiates immunotherapy in melanoma. Sci Transl Med 2017;9. doi: 10.1126/scitranslmed.aal4712.
33. Dieterich LC, Ducoli L, Shin JW, Detmar M. Distinct transcriptional responses of lymphatic endothelial cells to VEGFR-3 and VEGFR-2 stimulation. Sci Data 2017;4:170106.
34. Zhang Y, Lu Y, Ma L, Cao X, Xiao J, Chen J, et al. Activation of vascular endothelial growth factor receptor-3 in macrophages restrains TLR4-NF-kappaB signaling and protects against endotoxin shock. Immunity 2014; 40:501–14.
35. Pagliari LJ, Perlman H, Liu H, Pope RM. Macrophages require constitutive NF-kappaB activation to maintain A1 expression and mitochondrial homeostasis. Mol Cell Biol 2000;20:8855–65.
36. Kang S, Lee SP, Kim KE, Kim HZ, Memet S, Koh GY. Toll-like receptor 4 in lymphatic endothelial cells contributes to LPS-induced lymphangiogenesis by chemotactic recruitment of macrophages. Blood 2009;113: 2605–13.
37. Ries CH, Cannarile MA, Hoves S, Benz J, Wartha K, Runza V, et al. Targeting tumor-associated macrophages with anti-CSF-1R antibody reveals a strategy for cancer therapy. Cancer Cell 2014;25: 846–59.
38. Kruse J, von Bernstorff W, Evert K, Albers N, Hadlich S, Hagemann S, et al. Macrophages promote tumour growth and liver metastasis in an orthotopic syngeneic mouse model of colon cancer. Int J Colorectal Dis 2013;28: 1337–49.
39. Hirakawa S, Brown LF, Kodama S, Paavonen K, Alitalo K, Detmar M. VEGF-C-induced lymphangiogenesis in sentinel lymph nodes promotes tumor metastasis to distant sites. Blood 2007;109:1010–7.
40. Saaristo A, Veikkola T, Enholm B, Hytonen M, Arola J, Pajusola K, et al. Adenoviral VEGF-C overexpression induces blood vessel enlargement, tortuosity, and leakiness but no sprouting angiogenesis in the skin or mucous membranes. FASEB J 2002;16:1041–9.
41. Hamrah P, Chen L, Cursiefen C, Zhang Q, Joyce NC, Dana MR. Expression of vascular endothelial growth factor receptor-3 (VEGFR-3) on monocytic bone marrow-derived cells in the conjunctiva. Exp Eye Res 2004;79: 553–61.
42. Hamrah P, Chen L, Zhang Q, Dana MR. Novel expression of vascular endothelial growth factor receptor (VEGFR)-3 and VEGF-C on corneal dendritic cells. Am J Pathol 2003;163:57–68.

Downloaded from cancerres.aacrjournals.org on February 26, 2020. © 2019 American Association for Cancer Research.

Published OnlineFirst June 25, 2019; DOI: 10.1158/0008-5472.CAN-18-3657

43. Grothey A, Van Cutsem E, Sobrero A, Siena S, Falcone A, Ychou M, et al. Regorafenib monotherapy for previously treated metastatic colorectal cancer (CORRECT): an international, multicentre, randomised, placebo-controlled, phase 3 trial. Lancet 2013;381:303–12.
44. Yoshino T, Komatsu Y, Yamada Y, Yamazaki K, Tsuji A, Ura T, et al. Randomized phase III trial of regorafenib in metastatic colorectal cancer: analysis of the CORRECT Japanese and non-Japanese subpopulations. Invest New Drugs 2015;33:740–50.
45. Van Cutsem E, Yoshino T, Hocke J, Oum'Hamed Z, Studeny M, Tabernero J. Rationale and design for the LUME-Colon 1 Study: a randomized, double-blind, placebo-controlled phase III trial of nintedanib plus best supportive care versus placebo plus best supportive care in patients with advanced colorectal cancer refractory to standard treatment. Clin Colorectal Cancer 2016;15:91–4.
46. Xu RH, Li J, Bai Y, Xu J, Liu T, Shen L, et al. Safety and efficacy of fruquintinib in patients with previously treated metastatic colorectal cancer: a phase Ib study and a randomized double-blind phase II study. J Hematol Oncol 2017;10:22.
47. Xu RH, Shen L, Wang KM, Wu G, Shi CM, Ding KF, et al. A randomized, double-blind, parallel-group, placebo-controlled, multicenter, phase II clinical study of famitinib in the treatment of advanced metastatic colorectal cancer. J Clin Oncol 2015;33:513.

Downloaded from cancerres.aacrjournals.org on February 26, 2020. © 2019 American Association for Cancer Research.

Published OnlineFirst June 25, 2019; DOI: 10.1158/0008-5472.CAN-18-3657

Cancer Research
The Journal of Cancer Research (1916–1930) | The American Journal of Cancer (1931–1940)

AACR American Association for Cancer Research

Activation of the VEGFC/VEGFR3 Pathway Induces Tumor Immune Escape in Colorectal Cancer

Carlotta Tacconi, Federica Ungaro, Carmen Correale, et al.

Cancer Res 2019;79:4196-4210. Published OnlineFirst June 25, 2019.

Updated version	Access the most recent version of this article at: doi:10.1158/0008-5472.CAN-18-3657
Supplementary Material	Access the most recent supplemental material at: http://cancerres.aacrjournals.org/content/suppl/2019/06/25/0008-5472.CAN-18-3657.DC1

Cited articles	This article cites 45 articles, 7 of which you can access for free at: http://cancerres.aacrjournals.org/content/79/16/4196.full#ref-list-1

E-mail alerts	Sign up to receive free email-alerts related to this article or journal.
Reprints and Subscriptions	To order reprints of this article or to subscribe to the journal, contact the AACR Publications Department at pubs@aacr.org.
Permissions	To request permission to re-use all or part of this article, use this link http://cancerres.aacrjournals.org/content/79/16/4196. Click on "Request Permissions" which will take you to the Copyright Clearance Center's (CCC) Rightslink site.

Downloaded from cancerres.aacrjournals.org on February 26, 2020. © 2019 American Association for Cancer Research.